CHAPTER VII
QUIESCENT AND SHEAR-INDUCED COLD CRYSTALLIZATION IN POLY(TRIMETHYLENE TEREPHTHALATE)

Phornphon Srimoaon, Pitt Supaphol*, and Anuvat Sirivat

The Petroleum and Petrochemical college, Chulalongkorn University, Soi Chula 12, Phyathai Road, Pathumwan, Bangkok 10330, THAILAND

ABSTRACT

Shear-induced crystallization in poly(trimethylene terephthalate) PTT was investigated via different scanning calorimetry (DSC). The shear treated samples were prepared both low and high shear rates region by cone and plate and capillary rheometer, respectively. The induction time of shear treated samples was found to be lower than that of shear untreated one. The peak temperature of cold crystallization of shear treated samples was also shifted to the lower temperature. The kinetic model of shear-induced crystallization stated that the polymer melt which has the effect of orientation would have a reduced amount of entropy as modified from quiescent crystallization. A non-linear regression method was used for directly fitting non-isothermal experimental data using the differential type of Nakamura model to obtain crystallization rate equation parameters for both shear and non-sheared conditions. At condition with a fixed heating rate, the degree of orientation determined reached a maximum value and showed a less dependent on increasing shear rate. The degree of orientation as a function of heating rate was found to decrease with increasing shear rate. Analysis of the data was also carried out based on the Avrami, Tobin, and Urbanovici–Segal models. The activation energy of shear untreated and shear treated PTT samples based on the Kissinger, Takhor, and Friedman methods was also discussed.

(**Key-words**: poly(trimethylene terephthalate); shear-induced crystallization)

---

* To whom correspondence should be addressed: Fax: +66-2215-4459; E-mail address: pitt.s@chula.ac.th

1. INTRODUCTION

In actual processings of a semicrystalline polymer, primary crystallization of a semicrystalline polymer, primary nucleation mechanism and rate are characterized and controlled not only by the presence of infusible heterogeneous nuclei (e.g. catalyst residues, nucleating agents, etc.), but the processing history (e.g. temperature, pressure, shear stress, etc.). So the resulting physical properties are strongly dependent on the morphology formed and the extent of crystallization during processing. The kinetics of crystallization of polymers in quiescent condition were extensively investigated by many observers but the effect of shear or stress is still incomplete because of difficulties in the experimental measurement and a crystallization kinetics model is not available.

Wolkowicz [1] studied the effect of shear on the melt crystallization behavior of poly (1-butene) at several shear rates and degree of under cooling. The shear stress in the system induced a certain amount of nucleation orientation which greatly accelerated the overall crystalline transformation process. Ness and Liang [2] investigated the influence of temperature and shear rate on flow behavior of HDPE melts during extrusion using capillary rheometer. They found that the phenomenon of shear-induced crystallization was easily produced when a die has a larger entry angle was used and the temperature was near the melting point of samples. Kim *et al.*[3] studied the memory effect of shear history of polyethylene terephthalate (PET) under shear conditions in a capillary rheometer. Double peaks of heating crystallization exotherms attributed to the existence of crystallization processes with different rates were observed. The effect of shear history was reduced because of the relaxation process during holding period in melt state before crystallization.

Eder *et al.*[4] proposed microscopic model for shear-induced crystallization under isothermal crystallization with a constant shear rate. They proposed that nucleation rate and growth rate were supposed to be functions of orientation function in the melt which was dependent on shear rate, shearing time and stress relaxation effect. Moitzi and Skalicki [5] developed Eder model to fits experimental results of isotactic polypropylene under isothermal crystallization with a constant shear rate. They suggested sheared polymer melts had a higher number of crystallization nuclei

than quiescent melts at the same crystallization. Jerschow and Janeschitz-Kriegl [6] studied about effect of long molecules in shear-induced crystallization of isotactic polypropylene by using nucleation model based on thread-like precursors which were formed during shear flow. From this experiment they found that the long polymer molecules had large effect for the formation of highly oriented layers due to shear treatment, and polypropylene with narrow molecular mass distributions had a lower tendency to form this structure.

Recently, Ahn *et al.* [7] studied shear-induced cold crystallization of poly(ethtylene terephthalate) PET under isothernal and non-isothermal conditions. The differential type of Nakamura model, which term nucleation constant K_g, modified with the degree of orientation, was used to fit the experimental results under non-isothermal condition. The kinetic model of shear-induced crystallization stated that the polymer melt which has the effect of orientation would have a reduced amount of entropy as modified from quiescent crystallization. Guo and Narh [8] proposed simplified model of stress-induced crystallization kinetics of PET under isothermal crystallization from the melt. The assumption of this model is that the effect of shear stress on crystallization can only increase the equilibrium melting temperature $T_m°$. The advantage of this model is that the parameters in quiescent state crystallization model do not change and can be determined easily. They found that shear stress applied not only increased the rate of crystallization, but also broadened the crystallization temperature range. The peak temperature at highest crystallization rate was also shifted to higher temperature with increasing shear stress.

Poly(trimethylene terephthalate) (PTT), a relatively new linear aromatic polyester, is a member of the polyester family with three methylene units in its chemical structure. The synthetic method of PTT was first reported by Whinfield and Dickson in 1941 [9], but it was not commercially available then due to the high production cost of one of the reactants, 1,3-propanediol. Since then, PTT is now commercially available and has been produced by Shell Chemicals under the tradename Corterra™.

There are many papers on crystallization of PTT, but a small number of paper reporting effect of stress or shear on crystallization behavior of PTT. The

objective of this work is to study the effect of shear on crystallization and to compare with experimental results in the quiescent conditions, in order to understand better on shear-induced crystallization.

In this manuscript, we focus on the effect of shear rate, shearing time, shearing temperature, and effect of heating rate on sheared samples comparing to quiescent condition using differential scanning calorimetry (DSC) for both isothermal and non-isothermal cold crystallizations, shear treated samples were prepared using cone and plate rheometer and capillary rheometers.

2. THEORETICAL BACKGROUND

2.1. Quiescent Crystallization Kinetics

The most common approach used to describe the overall isothermal crystallization kinetics is the Avrami equation [10-12]:

$$\theta(t) = 1 - \exp[(-K_a t)^{n_a}] \in [0,1] \qquad (1)$$

where K_a and n_a are the Avrami crystallization rate constant and the Avrami exponent, respectively. Usually, the Avrami rate constant K_a is written in the form of the composite Avrami rate constant k_a (i.e. $k_a = K_a^n$). k_a (the dimension of which is given in $(\text{time})^{-n}$) is not only a function of temperature, but also a function of the Avrami exponent n_a. As a result, use of K_a should be more preferable than use of k_a due partly to the facts that it is independent of the Avrami exponent n_a and its dimension is given in $(\text{time})^{-1}$. It should be noted that both K_a and n_a are constants specific to a given crystalline morphology and type of nucleation for a particular crystallization condition [13] and that based on the original assumptions of the theory, the value of the Avrami exponent n_a should be an integer ranging from 1 to 4.

In the study of non-isothermal crystallization using DSC, the energy released during the crystallization process appears to be a function of temperature rather than time as in the case of isothermal crystallization. As a result, the relative crystallization function of temperature $\theta(T)$ can be formulated as:

$$\theta(T) = \frac{\int_{T_0}^{T} \left(\frac{dH_c}{dT}\right) dT}{\Delta H_c} \qquad (2)$$

where T_o and T represent the onset and an arbitrary temperature, respectively, dH_c is the enthalpy of crystallization released during an infinitesimal temperature range dT, and ΔH_c is the overall enthalpy of crystallization for a specific cooling condition.

In an attempt to use Equation (1) to analyze the non-isothermal crystallization data in a DSC, we need to assume that the sample experiences the same thermal history as designated by the DSC furnace. This may be realized only when the thermal lag between the sample and the furnace is kept minimal. If this assumption is valid, the relation between the crystallization time t and the sample temperature T can be formulated as:

$$t = \frac{T_0 - T}{\phi} \tag{3}$$

where ϕ is the cooling rate. According to Equation (3), the horizontal temperature axis observed in a DSC thermogram for the non-isothermal crystallization data can readily be transformed into the time scale.

The important consideration for Avrami approach is that the model is only appropriate for the early stages of crystallization. The complications arise due to the effects of growth site impingement and secondary crystallization process, which were disregarded for the sake of simplicity in the original derivation of the model. A theory of phase transformation kinetics with growth site impingement was proposed by Tobin [14-16]. According to this approach, the equation of phase transition reads

$$\theta(t) = \frac{(K_t t)^{n_t}}{1 + (K_t t)^{n_t}} \in [0,1] \tag{4}$$

where K_t is the Tobin rate constant, and n_t the Tobin exponent. Based on this proposition, the Tobin exponent needs not be integral [14-16], and it is mainly governed by different types of nucleation and growth mechanisms. It should be noted that, according to the original applications , the Tobin rate constant is written in the form of the composite Tobin rate constant k_t (i.e. $k_t = K_t^n$), which is not only a function of time, but also a function of the Tobin exponent n_t (similar to the case of k_a mentioned previously). As a result, use of K_t should be more preferable than use of k_t due partly to the facts that it is independent of the Tobin exponent n_t and its dimension is given in $(\text{time})^{-1}$. Recently, Urbanovici and Segal [17] proposed a new macrokinetic equation, which is essentially a generalization of the Avrami model. In

this proposition, the relation between the relative crystallinity as a function of time $\theta(t)$ and the crystallization time t is written as:

$$\theta(t) = 1 - \left[1 + (r-1)(K_{us}t)^{n_{us}}\right]^{1/(1-r)} \in [0,1] \quad (5)$$

where K_{us} and n_{us} are the Urbanovici-Segal crystallization rate constant and the Urbanovici-Segal exponent, respectively. r is the parameter satisfying the condition $r > 0$. At the condition where $r \rightarrow 1$, the Urbanovici-Segal model becomes identical to the Avrami model [17]. This simply means that parameter r is merely the factor determining the degree of deviation of the Urbanovici-Segal model from the Avrami model. It is worth noting that both K_{us} and n_{us} have similar physical meanings to the Avrami kinetics parameters (i.e. K_a and n_a), and the dimension of K_{us} is also in $(\text{time})^{-1}$.

A number of mathematical methods [18-19] were proposed for analyzing the data obtained from non-isothermal thermoanalytical investigations of crystallization of glass-forming liquids. In case of non-isothermal crystallization experiment using DSC, the effective activation energy ΔE can be evaluated from methods such as those proposed by Kissinger [18] or Takhor [19]. The main objective of these methods is to find a finite relationship between the peak temperatures T_p obtained from non-isothermal crystallization exotherms and the heating rate ϕ used.

If variation of the peak temperature T_p with the heating rate ϕ exists, the effective activation energy ΔE can be evaluated based on plots of the following forms: (1) Kissinger method,

$$\frac{d[\ln(\phi/T_p^2)]}{d(1/T_p)} = -\frac{\Delta E}{R} \quad (6)$$

and (2) Takhor method,

$$\frac{d[\ln(\phi)]}{d(1/T_p)} = -\frac{\Delta E}{R} \quad (7)$$

It is important to note that different assumptions utilized by these investigators during mathematical derivations for the sake of simplicity resulted in different relationships between T_p and ϕ, as evident in Equations (6) to (7).

For processes that occur on cooling, reliable values of the effective activation energy can be obtained, for instance, by the differential isoconversional method of Friedman [20]. The Friedman equation is obtained as follows:

$$\ln\left(\frac{d\alpha}{dt}\right)_{\alpha,i} = \ln[Af(\alpha)] - \frac{E_\alpha}{RT_{\alpha,i}} \tag{8}$$

where the subscript α denotes the values related to a given extent of conversion and i is the ordinal number of the run carried out at the heating rate, β_i.

Nakamura *et al.* [21] proposed a new model by simplifying Avrami model on the basis of isokinetic conditions and the assumption that the number of activated nuclei is constant. Nakamura developed the following equation from the Avrami theory:

$$\theta(t) = 1 - exp\left[-\left(\int_0^t K(T)dt\right)^n\right] \tag{9}$$

For process modeling, differential of Equation (9) and rearrange lead to the differential form of Nakamura equation which is frequently more useful than its integral form as following [22]:

$$\frac{d\theta}{dt} = nK(T)(1-\theta)[-\ln(1-\theta)]^{(n-1)/n} \tag{10}$$

where

$$K(T) = k(T)^{1/n} = (\ln 2)^{1/n}(t_{0.5}^{-1}) \tag{11}$$

$$t_{0.5}^{-1} = (t_{0.5}^{-1})_0 \exp\left(\frac{-U^*}{R(T-T_\infty)}\right)\exp\left(\frac{-K_g}{T\,\Delta Tf}\right) \tag{12}$$

where T is the crystallization temperature; n, the Avrami index; $t_{0.5}^{-1}$, reciprocal half-times of crystallization; $(t_{0.5}^{-1})_0$, a pre-exponential factor that include all terms independent of temperature; R, the universal gas constant; $\Delta T = T_m^\circ - T_c$, degree of undercooling; T_m°, the equilibrium melting temperature; $f = 2T/(T + T_m^\circ)$, a correction factor accounting for the reduction in the latent heat of fusion as the temperature is decreased; $T_\infty = T_g - 30$ K, the temperature below which transport ceases; T_g, the glass transition temperature; U^*, the activation energy for segmental jump rate in polymer; and K_g, the nucleation exponent. Equation (12) have often taken to have a similar temperature dependence to that of the subsequent crystal

growth rate G (written in the context of the original Lauritzen-Hoffmann secondary nucleation theory (LH theory) [23].

2.2 Shear-induced Crystallization Crystallization Kinetics

Ahn *et al.* [7] introduced the kinetic model of shear-induced crystallization containing with non-isothermal crystallization rate constant $K(T,\tau)$ as a function of temperature and shear stress.

Concept of the kinetic model of shear-induced crystallization started that polymer melt with orientation reduced a certain amount of entropy. So the orientation cause nuclei is easy to create thermodynamically. From original Hoffmann theory [23] the second exponential term can be written as another form by substituting K_g with:

$$K_g = \frac{\xi b_0 \sigma \sigma_e T_m^\circ}{k \Delta H_f^\circ} \tag{13}$$

where ξ equals 2 for regime II and 4 for regimes I and III (in this case use $\xi = 4$), b_0 denotes the crystal layer thickness along the growth direction, σ and σ_e are the lateral and fold surface free energies, respectively, T_m° is the equilibrium melting temperature, k is the boltzmann's constant, and ΔH_f° is the equilibrium heat of fusion:

$$K(T) = K_1 \exp\left(\frac{-U^*}{R(T-T_\infty)}\right)\exp\left(\frac{-4 b_0 \sigma \sigma_e}{kT}\cdot\frac{1}{\Delta f}\right) \tag{14}$$

where $\frac{1}{\Delta f} = \frac{T_m^\circ}{\Delta H_f^\circ \Delta T f}$ and Δf is the free energy of unoriented polymer. When the orientation of polymer chain occurs by flow, Δf was replaced with Δf_o as the free energy of oriented polymer [23]:

$$K(T) = K_1 \exp\left(\frac{-U^*}{R(T-T_\infty)}\right)\exp\left(\frac{-4 b_0 \sigma \sigma_e}{kT}\cdot\frac{1}{\Delta f_o}\right) \tag{15}$$

In the thermodynamic concept, free energy change Δf, can be expressed in two ways when polymer melt is changed to a crystalline.

1) the quiescent crystallization

$$\Delta f = \Delta H_f - T(S_m - S_c) \tag{16}$$

2) the sheared-induced crystallization

$$\Delta f_o = \Delta H_{f,o} - T(S_o - S_c) \quad (17)$$

where ΔH_f is the heat of fusion of the unoriented polymer melt, $\Delta H_{f,o}$ is the heat of fusion of the oriented polymer melt, S_m is the entropy of the unoriented polymer melt, S_o is the entropy of the oriented polymer melt, S_c is the entropy of the crystalline part.

Using assumption that $\Delta H_f = \Delta H_{f,o}$, so the change of the free energy of the oriented can be described by Equation (18):

$$\Delta f_o = \Delta f + T(S_m - S_o) = \Delta f\left[1 + \frac{T(S_m - S_o)}{\Delta f}\right] \quad (18)$$

In Equation (18) , changes in free energy in the case of the oriented are assumed to be expressed the modification of entropy. To reduce Equation (18), another function of temperature and shear stress, $h(T,\tau)$ was defined and shown in Equation (19)

$$h(T,\tau) = \frac{T(S_m - S_o)}{\Delta f} \quad (19)$$

So Equation(18) is equal to

$$\Delta f_o = \Delta f[1 + h(T,\tau)] \quad (20)$$

Substitution term in Equation (20) to (15). Finally, the kinetic model of shear-induced crystallization can be expressed as Equations (22) and (24) which are modified to crystallization rate constant $K(T,\tau)$ as a function of temperature and shear stress from Equations (10) to (12):

$$\frac{d\theta}{dt} = nK(T,\tau)(1-\theta)[-\ln(1-\theta)]^{(n-1)/n} \quad (21)$$

where

$$K(T,\tau) = K_i \exp\left(\frac{-U^*}{R(T - T_\infty)}\right)\exp\left(\frac{-K_g}{T\Delta Tf}\cdot\frac{1}{1+h(T,\tau)}\right) \quad (22)$$

For overall rate crystallization

$$K(T,\tau) = k(T,\tau)^{1/n} = (\ln 2)^{1/n}(t_{0.5}^{-1}) \quad (23)$$

$$t_{0.5}^{-1} = (t_{0.5}^{-1})_0 \exp\left(\frac{-U^*}{R(T - T_\infty)}\right)\exp\left(\frac{-K_g}{T\Delta Tf}\cdot\frac{1}{1+h(T,\tau)}\right) \quad (24)$$

3. EXPERIMENTAL

3.1. Material

Poly(trimethylene terephthalate) (PTT) were supplied in pellet form by Shell Chemical Company (USA) Ltd. (Corterra CP509201). The weight- and number-average molecular weight of this resin were determined to be ca. 78,100 and 34,700 Daltons, respectively. It should be noted that molecular weight characterization of these resins was carried out by Dr. Hoe Chuah and his co-workers of Shell Chemicals (USA) based on size-exclusion chromatography (SEC) technique.

3.2. Sample Preparation

For zero shear rate sample, PTT pellets clear grade were dried in a vacuum oven at 140°C for 5 hours prior to further use. A film of approximately 200 μm in thickness for each resin was melted-pressed at 260°C for PTT in Wabash V50H compression molding machine under an applied pressure of 4.62×10^2 $MN\cdot m^{-2}$. After 5 min holding time, the film was taken out and allowed to cool at the ambient condition down to room temperature between the two metal platens. This treatment assumes that previous thermo-mechanical history was essentially erased, and provided a standard crystalline memory condition for the as-prepared film.

For low shear rate samples, PTT pellets were dried in the oven at 140°C for 5 hours. Then the pellets were put into the mold which circle geometry to compress into the disk shape samples following by shearing samples using an ARES rheometer (Rheometrics Scientific, Inc.). The disk shape samples were inserted between cone and plate geometry and heated up to a desired fusion temperature T_f at 250°C. When the sample was melted completely, the excess sample was squeezed out and held until the temperature was equilibrated. Before beginning the test, the gap was set at exactly distance of 0.051 mm. When the equilibrium temperature was reached, the experiment was started in the transient mode. The shear rate used were 5 and 10 s^{-1} with different shearing times of 1, 3, and 5 min for both shear rates. After the cessation of shear, the sample was quenched immediately in liquid nitrogen bath to freeze the molecular structure of polymer before studying crystallization behavior with DSC technique.

For high shear rate samples, PTT pellets were dried in the oven at 140°C for 5 hours. before filling in the barrel of capillary rheometer. A capillary rheometer (Instron, model 4303) was used to applied shear stress to polymer samples before studying shear-induced crystallization with DSC technique. The diameter of die and L/D ratio are 1.25 mm and 40.15, respectively. Preheat time used was about 10 min. When the shear treated sample were extruded pass through capillary die, they were cut and quenched immediately in liquid nitrogen bath. The shearing temperatures used in this work were 250 and 260°C at various shear rates.

3.3. Differential Calorimetry Measurements

In this experiment, a DSC (DSC-7, Perkin-Elmer) was used to follow isothermal crystallization and subsequent melting behavior of these polyester resins. Calibration for temperature scale was carried out using a indium standard ($T_m°$= 156.6 °C and $\Delta H_f° = 28.5\ J{\cdot}g^{-1}$) on every other run to ensure accuracy and reliability of the data obtained. To minimize thermal lag between polymer sample and DSC furnace, each sample holder was loaded which weighed around 8.0 ± 0.3 mg. It is worth noting that each sample was used only once and all the runs were carried out under nitrogen atmosphere to prevent extensive thermal degradation.

To prepare quenched sample at zero shear rate, PTT film was heated from 40 to 280°C at a heating rate of 80°C·min^{-1} to a fusion temperature T_f at 250 and 260°C for a holding period of 5 min. Then DSC pan which contained sample inside was removed as quickly as possible from DSC sample holder and immersed immediately in liquid nitrogen bath for 10 min. The DSC pan was inserted again to DSC sample holder and heated up to 260°C with different heating rates.

For low shear rate and high shear rate samples, they just were heated from 25°C to 260°C at different heating rates. Crystallization exotherms and subsequent melting endotherms were observed with the same method as PTT sample at shear rate 0 s^{-1}.

4. RESULTS AND DISCUSSION

4.1. Kinetics of Quiescent Crystallization

The crystallization exotherm of PTT at shear rate 0 s^{-1} for non-isothermal cold crystallization and relative crystallinity at a heating rate of 20°C·min^{-1} are presented in Figure 1. The open symbol represents a relative crystallinity as a function of temperature calculated and the solid line represent the fitting result using differential Nakamura model, Equations (10) to (12).

The non-isothermal data can be fitted using n, $(t_{0.5}^{-1})_0$, and K_g as parameters of model while keeping U^* = 1500cal·mol^{-1}. The non-linear regression analysis of the data gave values of n, $(t_{0.5}^{-1})_0$, and K_g to be 2.43, 1.26×10^7 min^{-1}, and 9.68×10^4 K^2, respectively. The glass transition temperature T_g and equilibrium melting temperature T_m°used are 44 and 243.6°C [24], respectively. It is shown that differential type of Nakamura model fit well with the experimental data as shown with correlation coefficient r^2 = 0.9992.

4.2. Effect of Shear on Crystallization Behavior on Shear Treated Samples

4.2.1. Low Shear Rate Region

Figure 2 illustrates a result of the cold crystallization behavior comparing between PTT shear untreated and shear treated samples at low shear rate region, 5 and 10 s^{-1} with varies shearing times of 1, 3, and 5 min, and at a heating rate of 20°Cmin^{-1}. The peak temperature of cold crystallization T_{cc} of shear untreated sample is higher than that of shear treated sample at 5 and 10 s^{-1}. For the effect of shearing time, T_{cc} of sheared sample at 5 s^{-1} did not change when the shearing time increase from 1 to 5 min. The glass transition temperature T_g of shear untreated sample was found to be ca. 44°C which a little higher than that of the average value of the all low shear treated sample which was ca. 43.4 ± 1.24°C. Interestingly, the average value of onset of cold crystallization for all shear treated samples (i.e., 67.3 ± 1.41°C) started at lower temperature than that of shear untreated sample (i.e., 71.5°C) and the characteristic of cold crystallization peak of shear treated sample at 5 s^{-1} is shown with a broader peak. For shear treated sample at 10 s^{-1}, T_{cc} was shifted slightly to a lower temperature when shearing time increased from 1 to 5 min. The enthalpy of cold crystallization ΔH_c of shear treated sample at 5 and 10s^{-1} at different shearing time was lower than that of shear untreated sample (i.e. ΔH_c of shear

untreated and the average value of the shear treated sample 5 and 10 s^{-1} at all samples were 27.9 and 25.2 ± 0.65). For the peak of melting T_m and enthalpy of fusion $\Delta H_f°$ observed were found to increase with increasing shear rate and shearing time.

To confirm that the shift of cold crystallization peaks T_{cc} come from the orientational effect from shearing step before quenching samples, all of PTT shear treated samples at 5 and 10 s^{-1} were hold at fusion temperature T_f at 260°C for a fixed holding time t_h for 10 min after observing T_{cc} from heating scan. Then DSC pan which contained sample inside was removed as quickly as possible from DSC sample holder and immersed immediately in liquid nitrogen bath for 10 min. The DSC pan was inserted again to DSC sample holder and heated up to 260°C with a heating rate of 20°Cmin^{-1}. It was found that T_{cc} of second heating scan was ca. 74.5 ± 0.36°C for the average value of both shear rate 5 and 10 s^{-1}, respectively, which is higher than that of first heating scan. Moreover, the values of T_{cc} second heating scan of both shear rate 5 and 10 s^{-1} samples almost were the same value as non-sheared sample. From this experiment, we can conclude that the effect of molecular orientation from shearing step of cold crystallization would be lost when the samples were remelted before second quenching in studying cold crystallization.

4.2.2. High Shear Rate Region

The glass transition temperature T_g of shear untreated sample was found to be ca. 44 and 45.6°C for PTT samples at fusion temperatures of 250 and 260°C which are lower than that of the average value of the all low shear treated samples which were ca. 46.2 ± 2.84 and 48.5 ± 2.80°C for PTT at T_s 250 and 260°C. Interestingly, the average value of onset of cold crystallization for all shear treated samples (i.e., 66.8 ± 1.05°C and 68.4 ± 1.43 at T_s 250 and 260°C, respectively) was at lower temperature than that of shear untreated sample. Figure 3 illustrates cold crystallization behavior by comparing heat flows between shear untreated and high shear treated samples at various high shear rates. This figure also included low sheared samples at 5 and 10 s^{-1} at fixed shearing time for 1 min for comparison. The peak temperature of cold crystallization T_{cc} at shearing temperature T_s at 250°C also occurs at lower temperature , similar to the case of low shear rate samples at 5 and 10

s^{-1}. The change of T_{cc} of shear treated samples at various shear rates for different T_s is also summarized in Table 1. PTT high shear rate samples were also checked for the origin of shift of T_{cc}, similar to the case of low shear rate samples. The peak temperature of cold crystallization T_{cc} of second heating of high shear rate samples was found to be ca. 74.1 ± 0.57°C on the average of shear treated samples which occurs at nearly the same temperature of non-sheared sample. Figure 4 also illustrates plot of peak temperature of cold crystallization of PTT non-sheared and sheared samples at shearing temperatures T_s of 250 and 260°C measured at a heating rate of 20°C·min^{-1}. The shearing temperature was found to have an effect on the shift of T_{cc} which lower shearing temperature shows a greater shifting of T_{cc}. The effect of shear shows a greater difference after shear rate at ca. 150 s^{-1}. Ahn *et al.* [7] also found that the maximum crystallization temperature of PET was shifted to a lower temperature as shear rate increased. As shear rate increased from 0 to 57 s^{-1}, the peak temperature of cold crystallization T_{cc} of PET was shifted from ca. 149.5 to 126.2°C, equivalent to temperature change of 23.3°C. Kim *et al.* [3] also found that the peak temperature of cold crystallization of PET was shifted from 154 to 133°C as shear rate increased from 0 to 1168 s^{-1}. At the same shear rate with different molecular weight, they suggested that the effect of molecular weight was not significant as shown the shift of T_{cc} only ca. 3°C. Comparing to PTT studied, as shear rate increased from 0 to 53.2 s^{-1} , T_{cc} was shifted from 74.3 to 70.7°C only a shift of 3.6°C. The effect of shear rate caused a shift of T_{cc} of PET greater than that of PTT. It may be contributed from the favor conformation to crystallize of polymer (i.e., PET, all-trans [9] and PTT, -T_2G_2- [25]). When PET melt was extruded passing through the capillary die and immediately quenched with liquid nitrogen, the molecular chain was stretched and after quenching, most conformation of PET should be most all-trans as well as PTT. So the effect of shear should induce crystallization of PET more than of PTT leading to higher shifting of T_{cc}.

4.3. Non-Isothermal Crystallization Kinetics

Figure 5 illustrated the relative crystallinity as a function of temperature of PTT for shear untreated and shear treated samples at various shear rates recorded at a

heating rate 20°C·min^{-1}. This shows that the shear treated samples can be crystallized at the lower temperature relative to that of with shear untreated sample. The Avrami, Tobin, and Urbanovici–Segal model were also used to determine crystallization kinetics parameters of PTT samples of non-isothermal crystallization data by converting temperature to time scale. The induction time t_i, crystallization half-time $t_{0.5}$, reciprocal crystallization half-time $t_{0.5}^{-1}$, crystallization kinetics parameters (i.e. K_a, n_a, K_t, n_t, K_{ur}, n_{ur}, r) of PTT samples at different T_s are summarized in Table 2. At the same shearing temperature T_s, the induction time t_0 and bulk crystallization rate parameters (i.e. $t_{0.5}^{-1}$, K_a, K_t, K_{ur}) from non-isothermal crystallization of most shear treated samples were found to be lower than that of shear untreated sample. This may affect the assumption of the model proposed by Ahn *et al.* [7] which only considered the effect of shear on nucleation. For the effect of shearing temperature T_s at the same holding time, we found that the sheared samples prepared at higher T_s showed higher induction time t_i than that at lower shearing temperature used while bulk crystallization rate parameters (i.e. $t_{0.5}^{-1}$, K_a, K_t, K_{ur}) did not show any the trend. Crystallization half-time $t_{0.5}$ and exponent of each model (i.e. n_a, n_t, n_{ur}) of non-sheared sample were found to be lower than those of most sheared samples for each shearing temperature. Ahn *et al.* [7] studied shear-induced crystallization of PET and found that the reciprocal crystallization half-time $t_{0.5}^{-1}$ of sheared sample was a little higher than that of non sheared sample. They also suggested that growth mechanism of PET of sheared and non-sheared samples showed a similar behavior, but a nucleation step was greatly different depending on shear rate applied. So the difference of shear treated and shear untreated samples should come from the difference in nucleation constant K_g.

4.4. Isothermal Cold Crystallization

Figure 6 shows isothermal crystallization exotherms of PTT shear untreated and sheared treated sample at crystallization temperature T_c at 60°C. As shear rate increased, the peak temperature of cold crystallization was shifted to the lower crystallization time. Figure 7 illustrates the relative crystallinity as a function of crystallization time of PTT samples. The Avrami, Tobin, and Urbanovici–Segal model were used to determine crystallization kinetics parameters of sheared and non-

sheared samples. The experimental data are shown as various symbols and the fitting results of Avrami, Tobin, and Urbanovici–Segal analysis are shown as the solid, dashed, and dotted lines, respectively. The induction time t_i, crystallization half-time $t_{0.5}$, reciprocal crystallization half-time $t_{0.5}^{-1}$, Crystallization kinetics parameters (i.e. K_a, n_a, K_t, n_t, K_{ur}, n_{ur}, r) are summarized in Table 3. The induction time t_i, crystallization half-time $t_{0.5}$, and exponent of each model (i.e. n_a, n_t, n_{ur}) from isothermal crystallization of all shear treated samples are lower than that of shear untreated sample while bulk crystallization rate parameters (i.e. $t_{0.5}^{-1}$, K_a, K_t, K_{ur}) are higher. It should be noted here that the result of isothermal crystallization of shear treated samples, in which bulk crystallization rates are greater than that of non sheared sample, does not agree with non-isothermal crystallization analysis as mentioned previously.

4.5. Numerical Simulation for Kinetic Model for Shear-induced Crystallization

Ahn *et al.* [7] suggested that the nucleation step show different characteristic depending on applied shear rate. In quiescent crystallization, K_g denotes the nucleation constant while $K_{g,o}$ refers to the nucleation constant of shear-induced crystallization

$$K_{g,o} = \frac{K_g}{1 + h(T,\tau)} \tag{25}$$

Rearranged Equation (24), Equation (25) was obtained

$$h(T,\tau) = \frac{K_g}{K_{g,c}} - 1 \tag{26}$$

To determine the degree of orientation $h(T,\tau)$, $(t_{0.5}^{-1})_0$ and U^* were fixed and used the same value as quiescent crystallization. So only two parameters, n and $K_{g,o}$ were used to obtain the best fit using the Marquart algorithm [26]. Figure 8 show the value of $h(T,\tau)$ as a function of shear stress of sheared samples at different shearing temperature T_s at 250 and 260°C. As shear rate increases, the value of $h(T,\tau)$ increases sharply at low shear stress region and gradually increases further (almost constant) at high shear stress region. The shearing temperature T_s used also affected to the value of degree of orientation; a lower shearing temperature yields a higher the degree of orientation. Ahn *et al.* [7] found the value of $h(T,\tau)$ was quite

constant at rather high shear stress when shear stress increased meaning the degree of shear-induced molecular orientation reach a limited value. It was ascribed that the nucleation became easier and faster because of entropy reduction. The fitting results from differential type of Nakamura model were also plotted as various lines in Figure 5. From this figure, the fitting line of sheared samples was fitted quite well with the experimental data as correlation coefficient shown. The values of $K_{g,0}$, n, $h(T,\tau)$, and r^2 are also summarized in Table 4. The nucleation constant of shear condition $K_{g,0}$ of all shear treated samples studied is lower than that of shear untreated sample. The lower values $K_{g,0}$ of sheared sample should be explained with shear condition using lower energy (i.e., Fold and lateral surface free energy for nucleation step (See Equation (13)). Ahn *et al.* [8] and Patel and Spruiell [27] used the value of Avrami index n = 2 for fitting experimental data using differential Nakamura model. In this manuscript, n and $K_{g,o}$ were used to be parameters in the model to determine $h(T,\tau)$. It should be noted here that the Avrami index n of fitting of sheared sample is lower than that of non sheared sample. For analysis of PTT shear treated sample at 92.1 s^{-1}, the value of Avrami index n = 2.43 (same value in quiescent condition) and n is a parameter gave a value of $K_{g,0}$ to be ca. 7.87×10^4 with r^2 = 0.9986 and 7.84×10^4 with r^2 = 0.9989, respectively. It should be noted here that using n is a parameter in model giving the same results as fixing n equal to value from quiescent state.

4.6. Effect of Heating Rate on Shear-induced Crystallization

Figure 9 illustrates crystallization exotherms of shear untreated and shear treated samples at 92.1 and 245.6 s^{-1}, respectively, with various heating rates 10, 20, 30, and 40°C·min^{-1}. The peak temperature of cold crystallization T_{cc} was shifted to the higher temperature as heating rate increased both shear untreated and shear treated samples. The enthalpy of cold crystallization ΔH_c of shear untreated and shear treated samples (not shown) were found to increase with increasing heating rate. At the same heating rate, the position of T_{cc} of shear treated sample was located at lower temperature than that of shear untreated sample and shifted to the lower temperature as shear rate increased. Figure 10 illustrates relative crystallinity as function of temperature of shear untreated non-isothermally crystallized at various

heating rate. The fitting results using differential type of Nakamura model which 3 parameters n, $(t_{0.5}^{-1})_0$, and K_g were fitted well to all experimental data which are shown as various lines. Relative crystallinity as a function of temperature of shear untreated and shear treated samples at a constant heating rate at 20°C·min^{-1} are shown in Figure 11.

Table 5 summarizes the effect of heating rate on the crystallization kinetics parameters n, $(t_{0.5}^{-1})_0$ and K_g obtained from fitting the experimental data of shear untreated sample and n, $K_{g,0}$ of sheared sample using differential type of Nakamura model. For shear untreated samples, as heating rate increased, the value of $(t_{0.5}^{-1})_0$ changed while the value of K_g tend to be increased. The value of r^2 was used to show the fitting efficient of the model.

Figure 12 illustrates the value of $h(T,\tau)$ as function of shear stress of shear untreated and shear treated samples at 92.1, 245.6 s^{-1} with various heating rates. As heating rate increases, the value of degree of orientation $h(T,\tau)$ decreases both sheared sample at 92.1 and 245.6 s^{-1} (also see in Table 5). It can be explained that when heating rate increases, the polymer chains have less time to crystallize leading to the lower value of the degree of orientation.

4.7. Effective Activation Energy Describing the Overall Crystallization Process

Figures 13a to 13b illustrate plots based on the Kissinger [18], and the Takhor [19] methods, respectively. The slopes of the least-square lines drawn through these data are equal to $-\Delta E/R$; thus, the effective activation energy ΔE can be calculated accordingly. The values of the effective activation energy ΔE for these samples are summarized in Table 6. On the other hand, values as estimated by the Kissinger method are lower than those as Takhor (i.e., ca. 151.0 and 156.8 kJ·mol^{-1} for shear untreated sample).

From our previous work, Supaphol *et al.* [29] reported the effective activation energy ΔE value for PTT from non-isothermal melt crystallization as estimated by use of the Ozawa kinetic results to be ca.-118.0 kJ·mol^{-1} for PTT. Comparing to our previous work, the activation energy of PTT shear untreated sample from glassy state using Kissinger and Takhor analysis is lower than that of

neat PTT sample from melt state using Ozawa analysis. Interestingly, from this work the effective activation energy ΔE was found to decrease with increasing shear rate for both Kissinger and Takhor analysis (i.e., from 151.0 to 141.6 as shear rate increased from 0 to 245.6 s^{-1} for Kissinger analysis). The plots of effective activation energy ΔE of PTT non-sheared and sheared sample as a function of melt conversion based on the Friedman method [20] are also shown in Figure 14. At the melt conversion α lower than 0.5, the value of ΔE of shear treated sample at 245.6 s^{-1} show the lowest value while the value of ΔE of shear treated at 0 and 92.1 s^{-1} are comparable. Surprisingly, ΔE of shear treated samples are higher than that of shear untreated sample after melt conversion ca. $\alpha = 0.5$. Comparing the result from Friedman method (using ΔE at $\alpha = 0.5$) with Kissinger and Takhor method, we found that the values of ΔE obtained from Friedman method gives much lower values than those from Kissinger and Takhor method (i.e., 97.1, 151.1, and 156.8 $kJ \cdot mol^{-1}$ from Friedman, Kissinger, and Takhor method, respectively, for shear untreated PTT sample).

5. CONCLUSIONS

The non-isothermal crystallization exotherms of sheared samples showed that the peak temperature of cold crystallization was shifted towards lower temperatures with increasing shear rate. The effect of shearing time was found to have less effect on the crystallization behavior. The shearing temperature was found to have a effect on the shift of T_{cc} which lower shearing temperature shown greater shifting of T_{cc}. The effect of molecular orientation from shearing step of cold crystallization would be lost when the samples were remelted before second quenching both low and high shear rate region. In non-isothermal cold crystallization, the induction time t_i and bulk crystallization rate parameters (i.e., $t_{0.5}^{-1}$, K_a, K_t, K_{ur}) from non-isothermal crystallization of shear treated samples are lower than that of shear untreated sample. In isothermal mode, induction time t_i, crystallization half-time $t_{0.5}$ and exponent of each model (i.e. n_a, n_t, n_{ur}) of shear treated samples were found to be lower than that of shear untreated sample while bulk crystallization rate parameters (i.e., $t_{0.5}^{-1}$, K_a, K_t, K_{ur}) shown higher values. As

shear rate increased, the value of degree of orientation $h(T,\tau)$ tended to increase sharply at low shear stress region and gradually increased further as shown less dependent of shear at high shear stress region. The shear treated sample prepared at lower shearing temperature showed the trend of higher $h(T,\tau)$. The peak temperature of cold crystallization T_{cc} was shifted to the higher temperature as heating rate increased for both sheared and non-sheared samples. The value of $h(T,\tau)$ was found to decrease as shear rate increased. The effective activation energy ΔE was found to decrease with increasing shear rate in both Kissinger and Takhor analysis. The values of ΔE obtained from Friedman method (at melt conversion = 0.5) gave much lower values than those from Kissinger and Takhor method. The values of ΔE based on Friedman method of shear treated samples showed higher value than that of shear untreated sample after melt conversion = 0.5.

6. ACKNOWLEDGMENTS

The authors wish to thank Dr. Hoe H. Chuah and his co-workers of Shell Chemical Company (USA) Ltd. for supply of PTT and for their kind assistance on molecular weight measurements on all of the polyester resins received. PS acknowledges a grant provided by Chulalongkorn University through the Development Grants for New Faculty/Researchers. Partial in-kind support from the Petroleum and Petrochemical College is also greatly acknowledged.

REFERENCES

[1] Wolkowicz MD, Ph.D. Dissertation in Polym Sci Eng 1983, Graduate school, University of Massachusetts.

[2] Ness JN and Liang JZ, J App Polym Sci 1993, 48, 557.

[3] Kim SP and Kim SC, Polym Eng Sci 1993, 33, 83.

[4] Eder G, Janeschitz-Kriegl H, Lidauer S, Progress Polym Sci 1990, 15, 629.

[5] Moitzi J and Skalicky P, Polymer 1993, 34, 3168.

[6] Jerschow P and Janeschitz-Kriegl H, Int Polym Proc 1997, 12, 72.

[7] Ahn SH, Cho CB, and Lee KY, J Reinf Plas and Comp 2002, 21, 617.

[8] Guo J and Narh KA, Adv PolymTech 2002, 21, 214.

[9] Chuah H, in John Scheirs and Timothy Long ed. "Modern Polyester", John Wiley.

[10] Avrami M, J Chem Phys 1939, 7, 1103.

[11] Avrami M, J Chem Phys 1940, 8, 212.

[12] Avrami M, J Chem Phys 1941, 9, 177.

[13] Wunderlich B, in "Macromolecular Physics," Vol.2, Academic Press, New York, 1976, p 147.

[14] Tobin MC, J Polym Sci – Polym.Phys 1974,12, 399.

[15] Tobin MC, J Polym Sci – Polym.Phys 1976, 14, 2253.

[16] Tobin MC, J Polym Sci – Polym.Phys 1977, 15, 2269.

[17] Urbanovici E, Segal E, Thermochim Acta 1990, 171, 87.

[18] Kissinger HE, J Res Nat Bur Stand 1956, 57, 217.

[19] Takhor RL, In "Advances in Nucleation and Crystallization of Glasses," American Ceramics Society: Columbus, 1971; 166.

[20] Friedman, J Polym Sci C, 1964-1965, 6, 183.

[21] Nakamura K, Katayama K, Amano T, J App Polym Sci, 1973, 17, 1031

[22] Chan TW, Isayev AI, Polym Eng Sci, 1994, 34, 461.

[23] Hoffman JD, Davis GT, Lauritzen JI Jr, in: N.B. Hannay (Ed.), Treatise on Solid state Chemistry, Vol. 3, Plenum Press, Newyork, 1976, Chapter 7.

[24] Ziabicki A, In "Fundamentals of Fiber Spinning," John Wiley & Sons, New York, 1976, pp 112-114.

[25] Dangseeyun N, Srimoaon P, Supaphol P, and Nithitanakul M, Polymer, submitted.

[26] Desborough IJ, Hall IH, and Neisser JZ, Polymer 1979, 20, 419.

[27] Constantinides A and Mostoufi N, In "Numerical Methods for Chemical Engineers with MATLAB Applications", Prentice Hall PTR, New Jersey, 1999, 507.

[28] Patel MR and Spruiell JE, Polym Eng Sci, 1991, 31, 730.

[29] Supaphol P, Dangseeyun N, Srimoaon P, Nithitanakul M, Thermochim Acta, Submitted.

CAPTION OF TABLES

CAPTIONS OF FIGURES

Figure 1 Non-isothermal cold crystallization exotherms of PTT without shear effect and relative crystallinity recorded at a heating rate of 20°C·min^{-1}.

Figure 2 Non-isothermal cold crystallization exotherms of PTT shear untreated and shear treated samples at 5 and 10 s^{-1} at three different shearing time.

Figure 3 Non-isothermal cold crystallization exotherms of PTT shear untreated and shear treated samples at low shear rates and high shear rate.

Figure 4 Plot of peak temperature of cold crystallization of PTT shear untreated and shear treated samples at shearing temperature 250 and 260°C recorded at a heating rate of 20°C·min^{-1}.

Figure 5 Relative crystallization function of PTT shear untreated and shear treated samples at different shear rate at a heating rate of 20°·min^{-1}.

Figure 6 Isothermal cold crystallization exotherms of PTT shear untreated and shear treated samples at a crystallization temperature at 60 °C.

Figure 7 Relative crystallization function of time of PTT isothermally cold crystallized at different shear rates.

Figure 8 Degree of orientation $h(T,\tau)$ as a function of shear stress for PTT shear treated samples at different shearing temperature T_s 250°C and 260°C.

Figure 9 Non-isothermal cold crystallization exotherms of PTT shear untreated and shear treated samples at 92.1 and 25.6 s^{-1}.

Figure 10 Relative crystallization function of temperature of PTT shear untreated sample non-isothermally cold crystallized at four different heating rates.

Figure 11 Relative crystallization function of shear untreated and shear treated PTT samples non-isothermally cold crystallized at heating rate of 20°C·min^{-1}.

Figure 12 Degree of orientation $h(T,\tau)$ as a function of shear stress for shear treated PTT samples at 92.1 and 245.6 s^{-1} at four different heating rate.

Figure 13 Determination of the effective activation energy ΔE describing the overall crystallization process for PTT at shear rate 0, 92.1, and 245.6 s^{-1}.

Figure 14 Determination of the effective activation energy ΔE as a function of melt Conversion.

Table 1 The peak tempearature of cold crystalliztion T_{cc} and subsequent melting endotherms of PTT samples at a heating rate of 20°C·min^{-1}

Shear Rate s^{-1}	Shear Stress Pa	T_{cc} °C	ΔH_c(-) J·g^{-1}	T_m °C	ΔH_f(+) J·g^{-1}
T_s 250°C					
0	0	74.3	27.9	227.3	59.9
5t1	6.10×10^{2}	73.0	26.1	227.7	61.4
5t3	6.37×10^{2}	73.0	24.9	227.7	63.3
5t5	6.97×10^{2}	73.3	25.8	229.0	59.9
10t1	1.57×10^{3}	72.0	24.8	228.3	62.7
10t3	1.34×10^{3}	70.7	24.4	229.0	63.1
10t5	1.28×10^{3}	70.0	24.9	228.0	63.8
53.2	2.24×10^{4}	70.7	27.8	228.0	60.8
62.7	2.49×10^{4}	70.7	28.5	227.3	62.6
66.5	2.59×10^{4}	71.0	28.0	228.3	58.5
84.9	2.68×10^{4}	71.3	28.2	227.4	60.2
92.1	2.99×10^{4}	68.7	28.1	228.0	60.7
94.0	2.93×10^{4}	70.3	28.3	226.7	62.1
99.8	3.39×10^{4}	70.7	28.3	228.0	59.9
133.0	4.11×10^{4}	69.3	28.5	228.0	60.7
245.6	6.62×10^{4}	68.3	28.9	227.7	64.0
250.6	6.85×10^{4}	69.3	28.3	227.3	62.7
429.9	1.11×10^{5}	69.0	28.6	227.0	64.0
438.6	1.15×10^{5}	69.0	29.0	227.7	62.7
T_s 260°C					
0	0	74.3	29.1	226.7	62.5
70.6	1.23×10^{4}	70.0	29.2	228.3	62.7
105.9	1.55×104	69.7	29.8	228.3	63.0
141.2	1.82×104	71.3	28.6	227.7	62.7
211.9	2.29×104	71.3	28.6	228.0	64.3
268.0	3.93×104	70.7	28.9	227.0	63.2
469.0	5.66×104	71.7	29.2	227.3	64.9

Table 2 Non-isothermal crystallization kinetics of PTT non-sheared and sheared samples based on Avrami, Tobin, Urbanovici–Segal analysis at a heating rate of 20°C·min^{-1}

shear rate s^{-1}	t_i min	$t_{0.5}$ min	$t_{0.5}^{-1}$ min^{-1}	K_a min^{-1}	n_a	r^2	K_t min^{-1}	n_t min^{-1}	r^2	K_{us} min^{-1}	n_{us} min^{-1}	r	r^2
T_c 250°C													
0	2.10	0.292	3.42	3.14	4.30	0.9997	3.48	6.75	0.9987	3.15	4.28	1.05	0.9996
5t1	1.73	0.630	1.59	1.48	4.71	0.9994	1.63	7.99	0.9970	1.48	4.71	1.00	0.9994
5t3	1.60	0.789	1.27	1.19	5.91	0.9990	1.28	9.24	0.9986	1.24	7.09	1.48	0.9990
5t5	1.63	0.761	1.31	1.24	6.34	0.9987	1.33	10.3	0.9981	1.28	7.40	1.36	0.9988
10t1	1.72	0.550	1.82	1.68	4.52	0.9993	1.84	7.39	0.9977	1.71	4.79	1.14	0.9992
10t3	1.73	0.516	1.94	1.79	4.57	0.9995	1.96	7.38	0.9978	1.88	5.47	1.46	0.9996
10t5	1.81	0.527	1.90	1.55	4.95	0.9991	1.69	8.32	0.9988	1.58	5.21	1.17	0.9995
53.2	1.72	0.573	1.75	1.63	6.39	0.9986	1.75	8.86	0.9997	1.66	6.27	1.27	0.9988
62.7	1.84	0.445	2.25	2.08	5.46	0.9990	2.26	8.06	0.9998	2.10	5.39	1.14	0.9992
66.5	1.87	0.434	2.30	2.13	5.40	0.9989	2.32	7.82	0.9998	2.18	5.36	1.27	0.9990
84.9	1.77	0.577	1.73	1.63	6.56	0.9993	1.75	9.83	0.9993	1.65	6.52	1.13	0.9993
92.1	1.60	0.582	1.72	1.57	5.85	0.9960	1.72	10.1	0.9974	1.79	10.6	2.97	0.9997
94.0	1.84	0.428	2.34	2.16	5.58	0.9990	2.33	5.10	0.9908	2.19	5.50	1.15	0.9991
99.8	1.82	0.465	2.15	1.99	5.80	0.9986	2.13	5.45	0.9921	2.03	5.85	1.22	0.9990
133.0	1.82	0.465	2.15	1.96	5.96	0.9980	2.10	7.68	0.9998	2.04	6.35	1.67	0.9991
245.6	1.80	0.363	2.75	2.49	4.21	0.9980	2.77	5.98	0.9997	2.56	4.10	1.26	0.9979
250.6	1.80	0.415	2.41	2.21	5.11	0.9984	2.42	7.11	0.9997	2.28	5.06	1.30	0.9989
429.9	1.73	0.446	2.24	2.05	4.57	0.9992	2.25	7.39	0.9992	2.08	4.50	1.11	0.9991
438.6	1.68	0.521	1.92	1.78	6.18	0.9985	1.92	8.65	0.9998	1.81	6.05	1.24	0.9986
T_c 260°C													
0	2.07	0.386	2.59	2.40	5.25	0.9986	2.61	7.24	0.9996	2.43	5.07	1.21	0.9990
70.6	1.75	0.511	1.96	1.82	6.17	0.9981	1.96	8.42	0.9996	1.85	5.99	1.26	0.9982
105.9	1.84	0.403	2.48	2.28	5.08	0.9977	2.44	4.68	0.9914	2.35	4.86	1.39	0.9977
141.2	1.87	0.446	2.24	2.08	5.83	0.9986	2.25	8.29	0.9997	2.12	5.89	1.29	0.9987
211.9	1.84	0.479	2.09	1.95	6.10	0.9860	2.10	8.42	0.9996	2.00	5.98	1.30	0.9987
268.0	1.90	0.382	2.62	2.41	4.97	0.9960	2.64	6.14	0.9985	2.45	4.89	1.16	0.9991
469.0	1.77	0.570	1.75	1.65	6.71	0.9981	1.76	8.86	0.9993	1.68	7.16	1.46	0.9981

Table 3 Isothermal crystallization kinetics of PTT non-sheared and sheared samples based on Avrami, Tobin, Urbanovici–Segal analysis at a crystallization temperature 60°C

shear rate	t_0	$t_{0.5}$	$t_{0.5}^{-1}$	K_a	n_a	r^2	K_t	n_t	r^2	K_{us}	n_{us}	r	r^2
s-1	min	min	min^{-1}	min^{-1}			min^{-1}			min^{-1}			
0	0.595	2.37	0.422	0.363	2.75	0.9987	0.426	4.24	0.9989	0.394	3.26	1.41	0.9997
66.5	0.340	0.996	1.00	0.858	2.50	0.9989	1.01	4.07	0.9991	0.959	3.16	1.56	0.9998
133.0	0.272	0.966	1.04	0.896	2.73	0.9993	1.05	4.40	0.9989	0.967	3.23	1.39	0.9999
250.6	0.153	0.522	1.92	1.57	2.06	0.9979	1.92	3.34	0.9997	1.82	2.81	1.64	0.9999

Table 4 Crystallization rate parameters in Nakamura model n, K_g and degree of orientation $h(T,\tau)$ of shear untreated and shear treated PTT samples

shear rate	Shear Stress	n	K_g	h	r^2
s^{-1}	Pa		$K^2(\times10^{-4})$		
T_c 250°C					
0	0	2.43	9.68	0	0.9992
5t1	6.10×10^{2}	1.50	8.17	0.185	0.9995
5t3	6.40×10^{2}	1.54	9.01	0.074	0.9989
5t5	7.00×10^{2}	1.72	8.90	0.088	0.9988
10t1	1.57×10^{3}	1.57	7.55	0.282	0.9992
10t3	1.34×10^{3}	1.51	6.04	0.603	0.9993
10t5	1.28×10^{3}	1.58	5.57	0.740	0.9984
53.2	2.24×10^{4}	2.00	6.62	0.461	0.9980
62.7	2.49×10^{4}	2.25	8.67	0.116	0.9982
66.5	2.59×10^{4}	2.14	6.76	0.432	0.9980
84.9	2.68×10^{4}	2.15	7.84	0.234	0.9967
92.1	2.99×10^{4}	1.60	4.16	1.33	0.9948
94.0	2.93×10^{4}	2.22	5.71	0.695	0.9983
99.8	3.39×10^{4}	2.14	6.27	0.544	0.9980
133.0	4.11×10^{4}	1.96	4.96	0.950	0.9971
245.6	6.62×10^{4}	1.44	3.24	1.99	0.9990
250.6	6.84×10^{4}	1.98	4.53	1.14	0.9973
429.9	1.11×10^{5}	1.72	3.79	1.56	0.9984
438.6	1.15×10^{5}	1.99	4.36	1.22	0.9977
T_c 260°C					
0	0	2.40	12.2	0	0.9978
70.6	1.23×10^{4}	2.09	8.64	0.494	0.9974
105.9	1.55×10^{4}	2.00	7.72	0.672	0.9965
141.2	1.82×10^{4}	2.31	9.70	0.330	0.9979
211.9	2.29×10^{4}	2.26	9.83	0.310	0.9979
268.0	3.93×10^{4}	2.16	8.79	0.468	0.9981
469.0	5.66×10^{4}	2.13	10.5	0.230	0.9973

Table 5 Crystallization rate parameters in Nakamura model n, $(t_{0.5}^{-1})_0$, K_g and degree of orientation $h(T,\tau)$ of shear untreated and shear treated PTT samples at four different heating rate

Shear Rate (s^{-1})	0				92.1				245.6			
heating rate °C min^{-1}	n	$(t_{0.5}^{-1})_0$ min^{-1}	K_g K^2	r^2	n	K_g K^2	h	r^2	n	K_g K^2	h	r^2
10	2.40	1.43×10^7	6.90×10^4	0.9986	1.68	6.24×10^3	3.89	0.9968	1.59	8.98×10^3	2.21	0.9950
20	2.43	1.26×10^7	9.68×10^4	0.9992	1.78	3.44×10^4	1.33	0.9948	1.85	3.08×10^4	1.99	0.9990
30	2.28	2.38×10^7	1.27×10^5	0.9984	1.79	6.81×10^5	0.865	0.9973	1.22	4.71×10^4	1.69	0.9975
40	2.29	1.56×10^7	1.08×10^5	0.9987	1.80	7.06×10^4	0.530	0.9969	1.90	7.98×10^4	0.353	0.9970

Table 6 Effective activation energy ΔE describing the overall crystallization process of shear untreated and shear treated PTT samples

	Activation Energy ΔE (kJ $\cdot$mol^{-1})	
Shear rate (s^{-1})	Kissinger	Takhor
0.0	151.0	156.8
92.1	148.6	154.3
245.6	141.6	147.2

Table 7 Effective activation energy ΔE describing the overall crystallization process of shear untreated and shear treated PTT samples based on Friedman method

	Activation Energy ΔE (kJ mol-1)				
Shear Rate	$\alpha = 0.1$	$\alpha = 0.3$	$\alpha = 0.5$	$\alpha = 0.7$	$\alpha = 0.9$
0	148.9	116.4	97.1	89.8	113.6
92.1	148.9	117.0	104.8	113.0	138.9
245.6	134.0	105.6	105.6	146.5	235.9

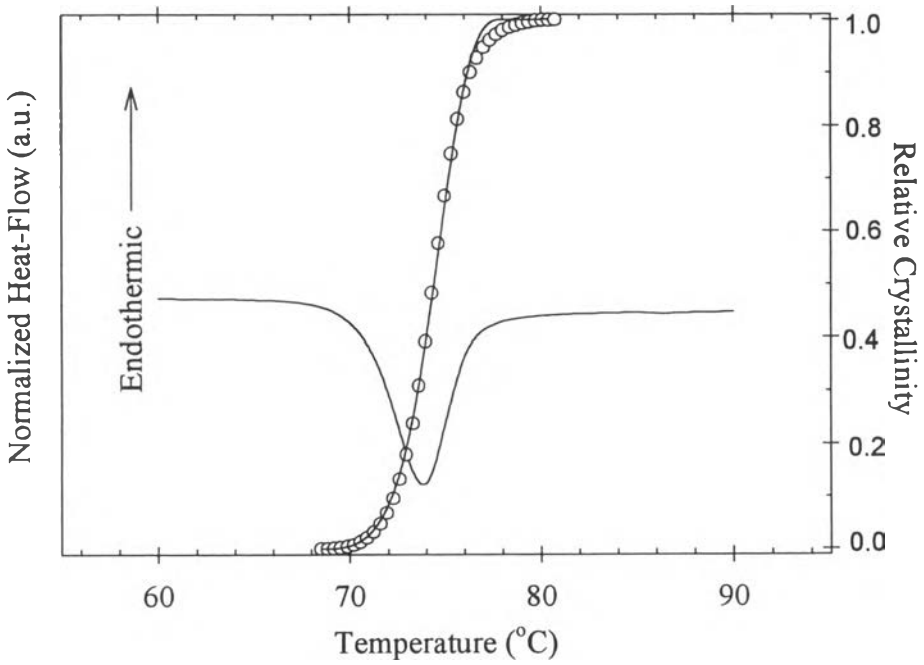
Normalized Heat-Flow (a.u.)
Endothermic
Relative Crystallinity
1.0
0.8
0.6
0.4
0.2
0.0
60
70
80
90
Temperature (°C)

Figure 1

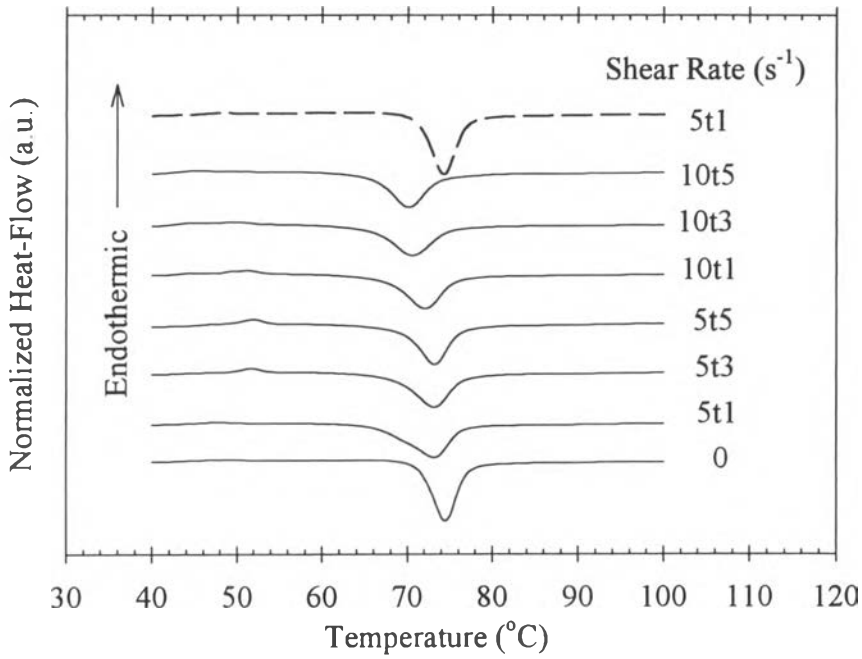
Shear Rate (s^{-1})
5t1
10t5
10t3
10t1
5t5
5t3
5t1
0
Endothermic
Normalized Heat-Flow (a.u.)
30
40
50
60
70
80
90
100
110
120
Temperature (°C)

Figure 2

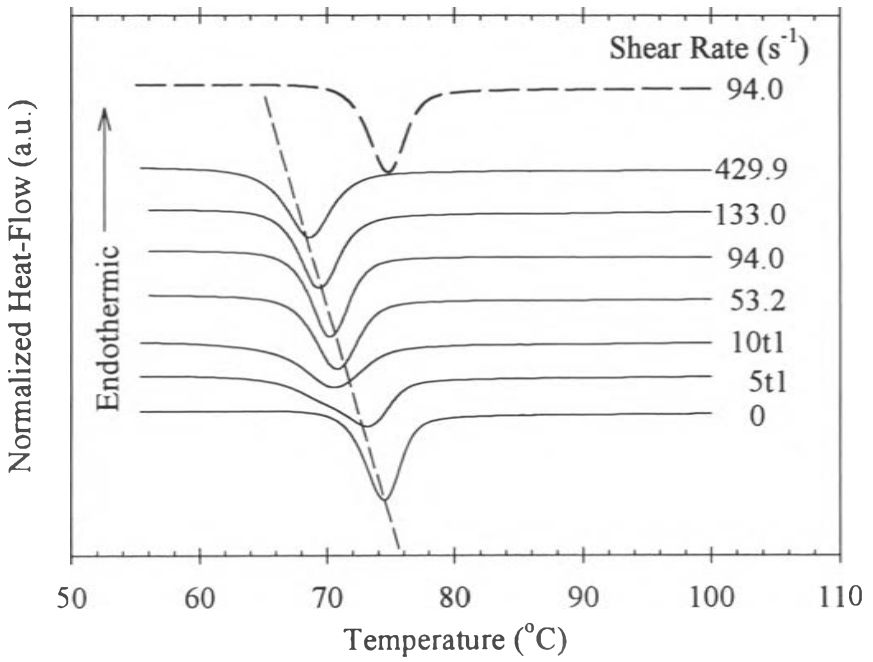
Shear Rate (s^{-1})
94.0
429.9
133.0
94.0
53.2
10t1
5t1
0
Endothermic
Normalized Heat-Flow (a.u.)
50
60
70
80
90
100
110
Temperature (°C)

Figure 3

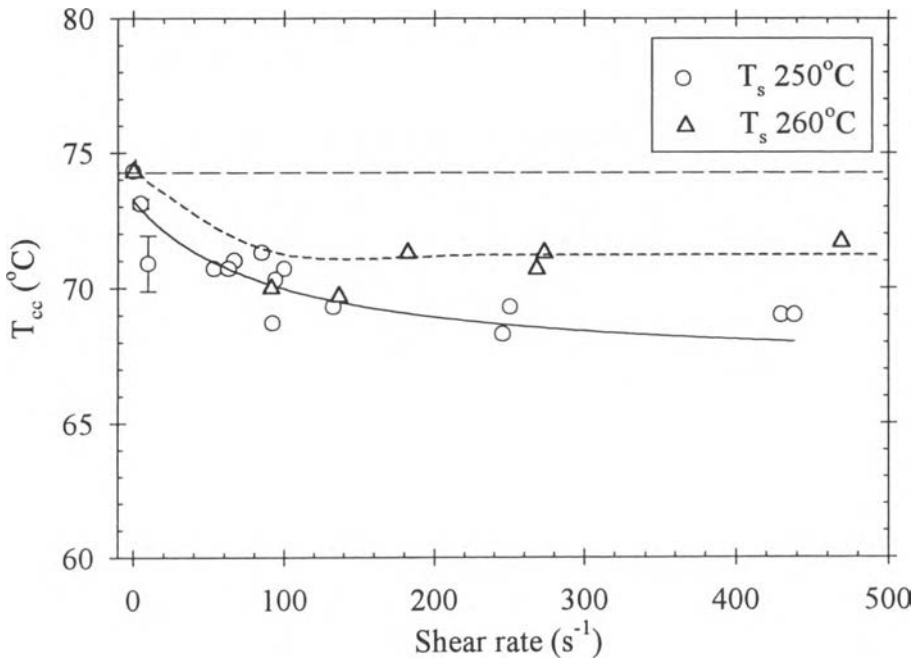
80
75
70
65
60
0
100
200
300
400
500
T_{cc} (°C)
Shear rate (s^{-1})
T_s 250°C
T_s 260°C

Figure 4

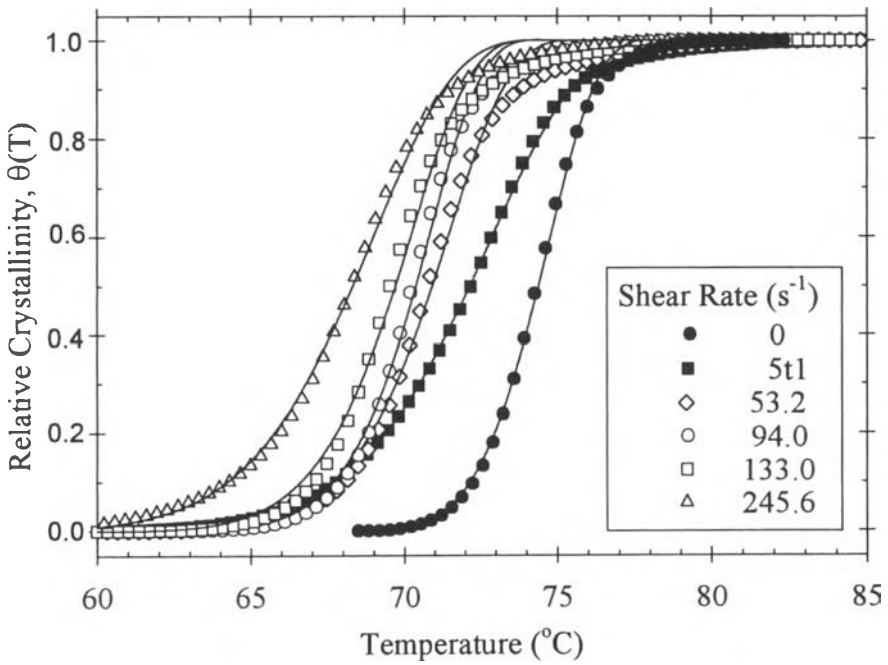
Relative Crystallinity, θ(T)
1.0
0.8
0.6
0.4
0.2
0.0
60
65
70
75
80
85
Temperature (°C)
Shear Rate (s-1)
0
5t1
53.2
94.0
133.0
245.6

Figure 5

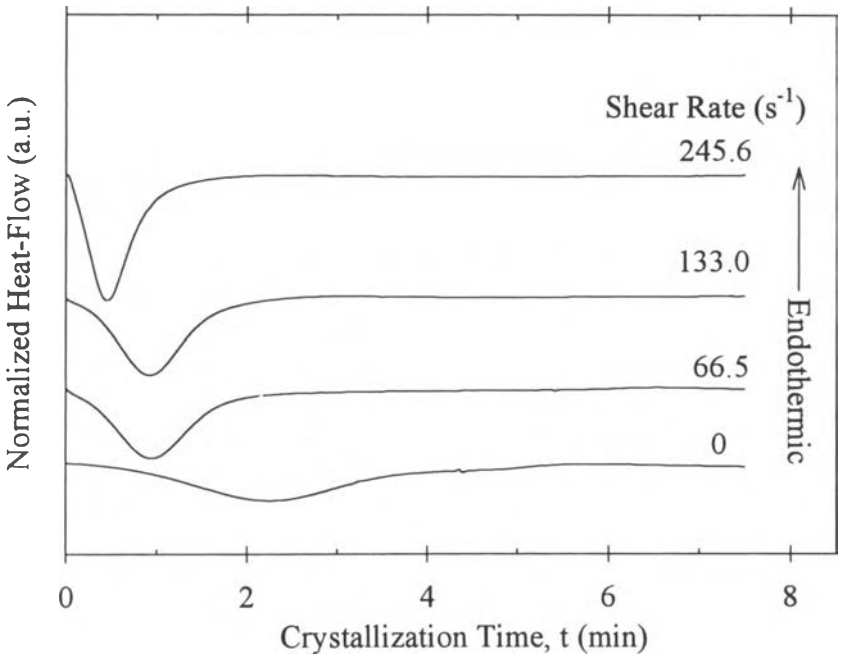
Shear Rate (s^{-1})
245.6
133.0
66.5
0
Endothermic
Normalized Heat-Flow (a.u.)
0
2
4
6
8
Crystallization Time, t (min)

Figure 6

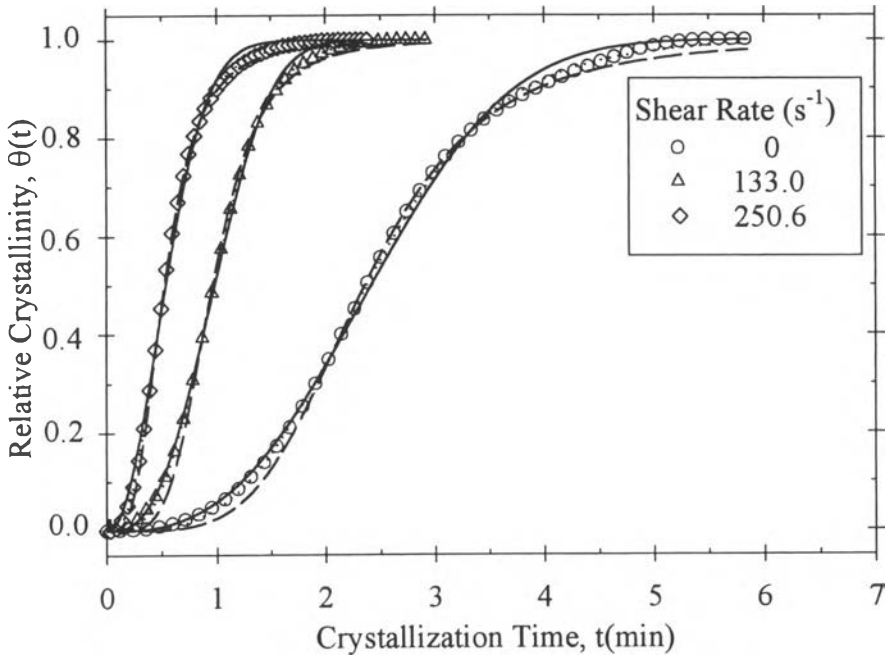
Relative Crystallinity, θ(t)
1.0
0.8
0.6
0.4
0.2
0.0
0
1
2
3
4
5
6
7
Crystallization Time, t(min)
Shear Rate (s-1)
0
133.0
250.6

Figure 7

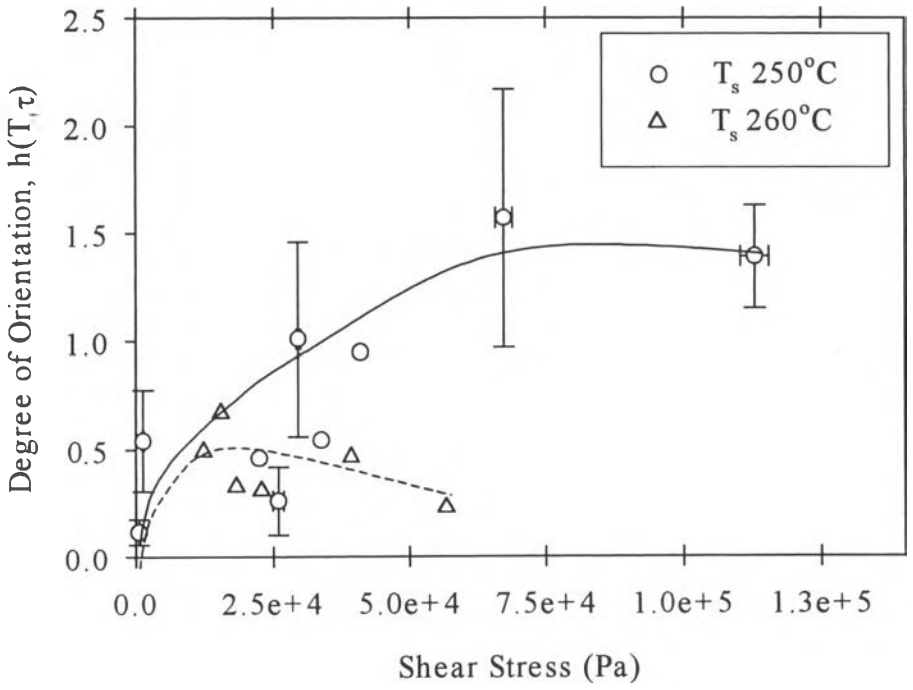

Figure 8

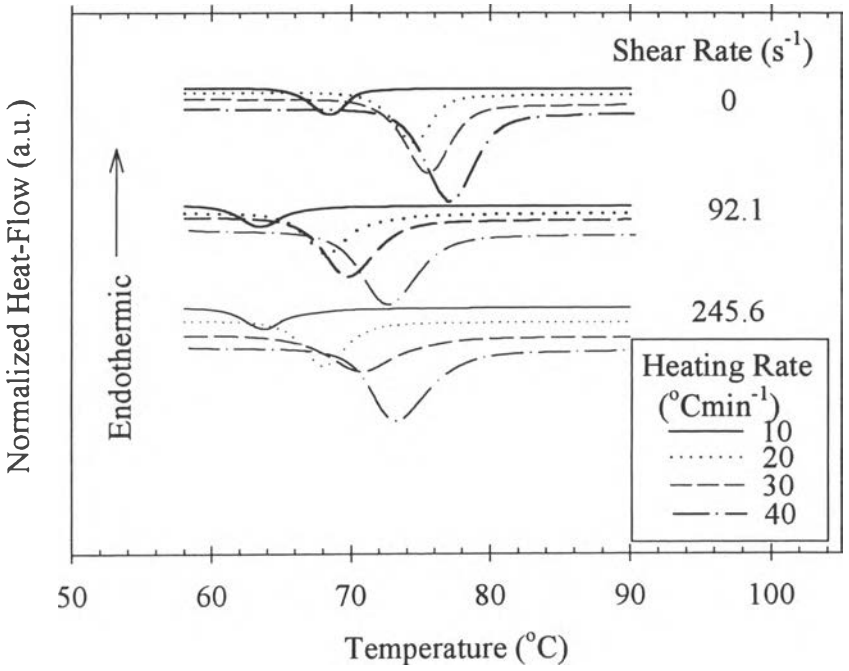
Shear Rate (s^{-1})
0
92.1
245.6
Heating Rate
($^{o}Cmin^{-1}$)
10
20
30
40
Endothermic
Normalized Heat-Flow (a.u.)
50
60
70
80
90
100
Temperature (^{o}C)

Figure 9

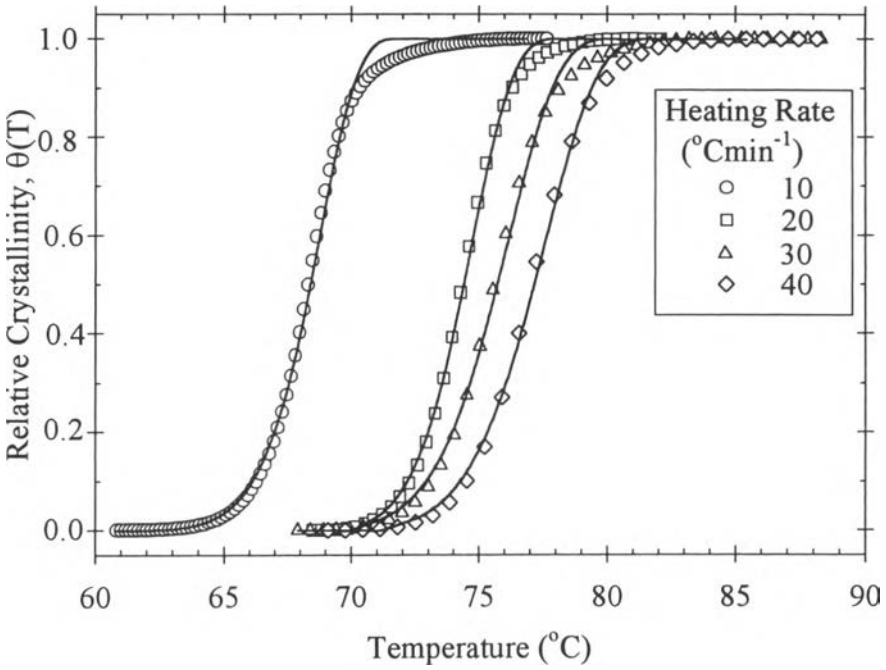
Relative Crystallinity, θ(T)
1.0
0.8
0.6
0.4
0.2
0.0
60
65
70
75
80
85
90
Temperature (°C)
Heating Rate
(°Cmin-1)
10
20
30
40

Figure 10

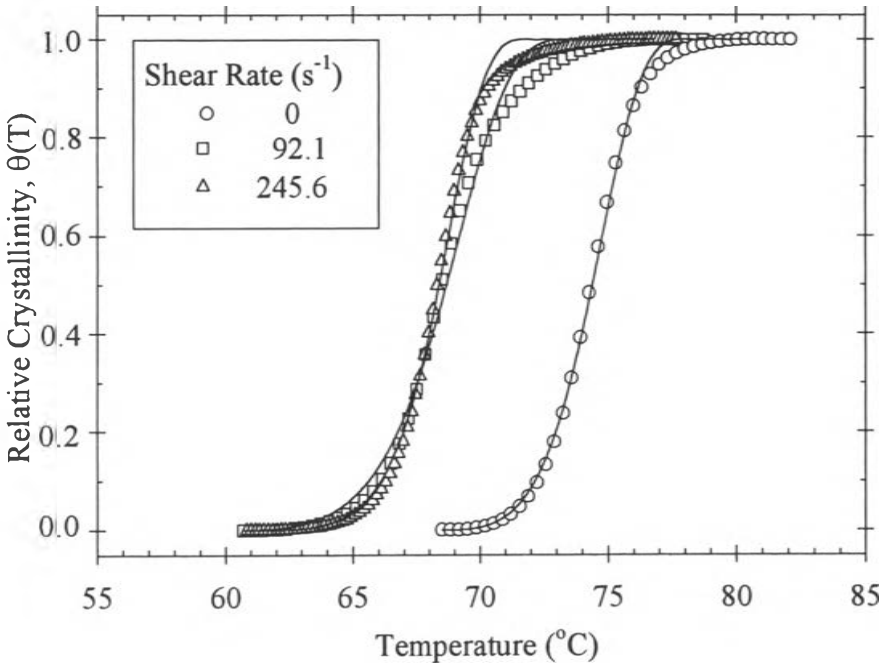
Shear Rate (s^{-1})
0
92.1
245.6
Relative Crystallinity, θ(T)
1.0
0.8
0.6
0.4
0.2
0.0
55
60
65
70
75
80
85
Temperature (°C)

Figure 11

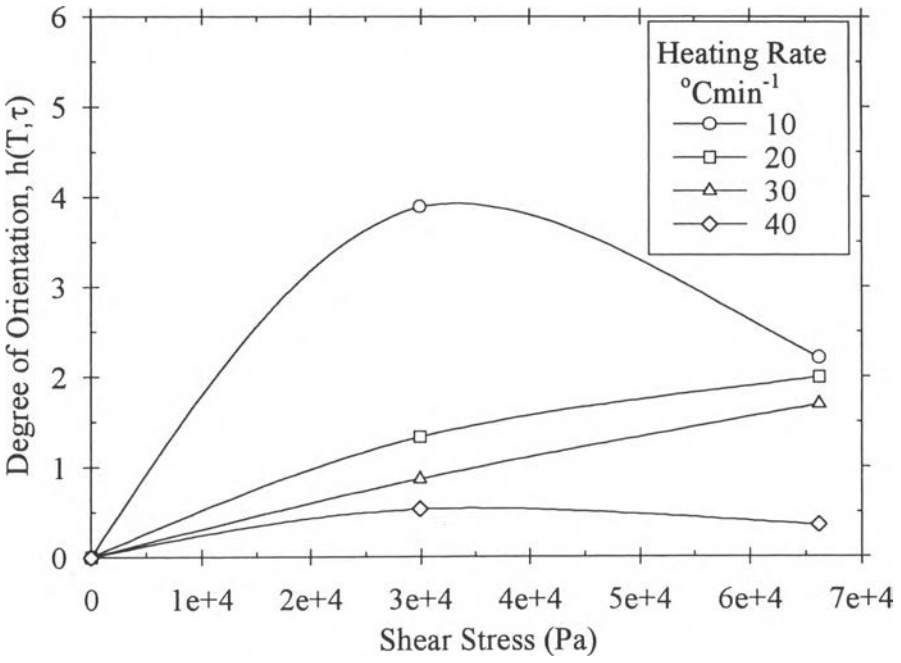
Degree of Orientation, h(T,τ)
Shear Stress (Pa)
Heating Rate
°Cmin-1
10
20
30
40
0
1
2
3
4
5
6
0
1e+4
2e+4
3e+4
4e+4
5e+4
6e+4
7e+4

Figure 12

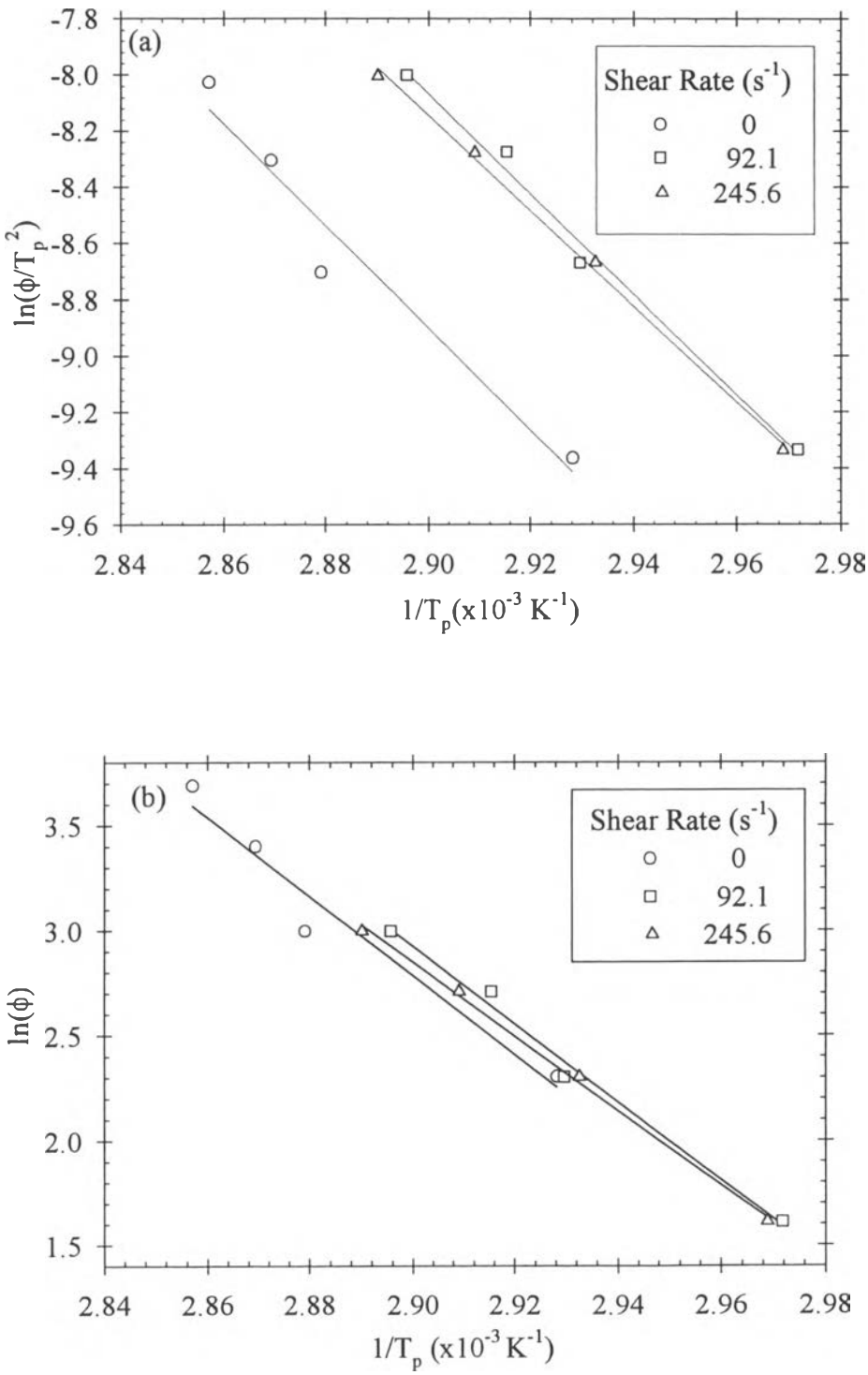
(a)
Shear Rate (s^{-1})
0
92.1
245.6
$\ln(\phi/T_p^2)$
$1/T_p(x10^{-3}\ K^{-1})$
(b)
Shear Rate (s^{-1})
0
92.1
245.6
$\ln(\phi)$
$1/T_p\ (x10^{-3}\ K^{-1})$

Figure 13

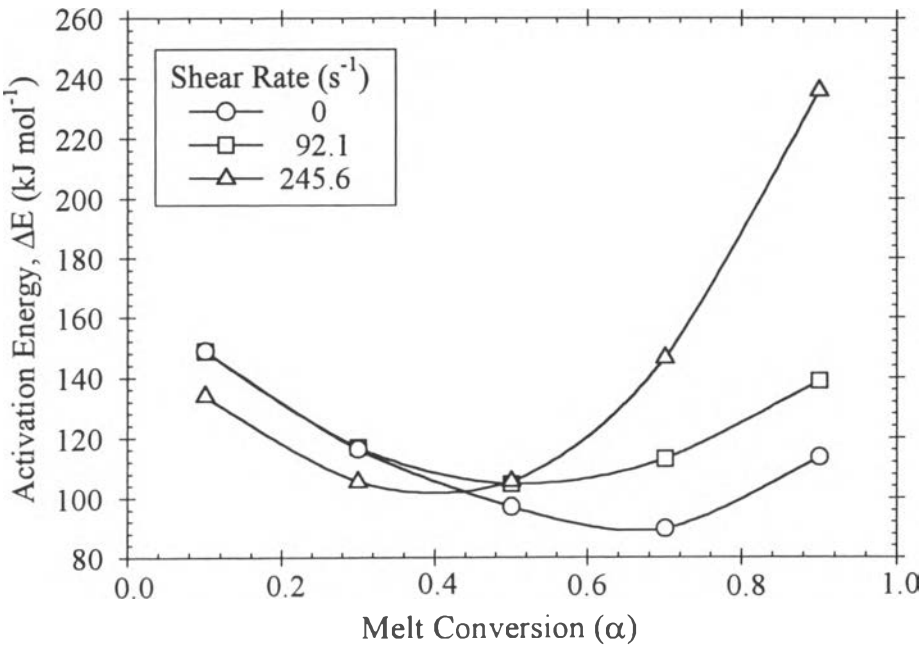
Shear Rate (s^{-1})
0
92.1
245.6
Activation Energy, ΔE (kJ mol^{-1})
Melt Conversion (α)
260
240
220
200
180
160
140
120
100
80
0.0
0.2
0.4
0.6
0.8
1.0

Figure 14